GSI

GSI-Preprint-97-60
Oktober 1997

A LARGE AREA SCINTILLATING FIBER DETECTOR FOR RELATIVISTIC HEAVY IONS

J. Cub, G. Stengel, A. Grünschloß, K. Boretzky, T. Aumann, W. Dostal, B. Eberlein, Th. W. Elze, H. Emling, G. Ickert, J. Holeczek, R. Holzmann, J. V. Kratz, R. Kulessa, Y. Leifels, H. Simon, K. Stelzer, J. Stroth, A. Surowiec, E. Wajda

(To be published in Nucl. Instruments and Methods in Phys. Res. A)

Gesellschaft für Schwerionenforschung mbH
Planckstraße 1 • D-64291 Darmstadt • Germany
Postfach 11 05 52 • D-64220 Darmstadt • Germany

A Large Area Scintillating Fiber Detector for Relativistic Heavy Ions

J. Cub [b,e], G. Stengel [a], A. Grünschloß [a], K. Boretzky [a], T. Aumann [c], W. Dostal [c], B. Eberlein [c], Th.W. Elze [a], H. Emling [b], G. Ickert [b], J. Holeczek [b], R. Holzmann [b], J.V. Kratz [c], R. Kulessa [d], Y. Leifels [b], H. Simon [e], K. Stelzer [a], J. Stroth [a], A. Surowiec [b], E. Wajda [d]

[a] *Institut für Kernphysik, Universität Frankfurt, D-60486 Frankfurt, Germany*

[b] *Gesellschaft für Schwerionenforschung, D-64291 Darmstadt, Germany*

[c] *Institut für Kernchemie, Universität Mainz, D-55029 Mainz, Germany*

[d] *Instytut Fizyki, Uniwersytet Jagielloński, PL-30-059 Kraków, Poland*

[e] *Institut für Kernphysik, Technische Hochschule Darmstadt, D-64289 Darmstadt, Germany*

A scintillating fiber detector for relativistic heavy ions with an active area of 50×50 cm^2 has been developed and was tested with various ion beams ($1 \leq Z \leq 92$). At count rates of up to 10^5 particles/s, the position resolution was found to be determined by the fiber width of 1 mm; depending on the nuclear charge of the beam, efficiencies between 89% and 100% and time resolutions between 800 and 200 ps (FWHM) were obtained.

1 Introduction

During the past few years, invariant-mass spectroscopy after heavy-ion projectile break-up reactions at near relativistic beam energies has developed into a very valuable tool for nuclear spectroscopy purposes. This concerns, in particular, the investigation of high-lying nuclear resonances (e.g. multiphonon giant resonances [1]) or applications with secondary radioactive beams (e.g. [2]). Such kinematically complete measurements require to reconstruct the trajectory of the heavy fragments in order to determine scattering angles and nuclear mass numbers. The nuclear mass numbers can be determined via the deflection angle of the ions traversing a dipole magnet if, in addition, the nuclear charge and the velocity of the ions are obtained via energy loss (ΔE)

and via time-of-flight (ToF) measurements, respectively. In order to cope with the requirements of different types of experiments using relativistic heavy ions a position-sensitive detector is required, covering a large area with a position resolution of about 1 mm and the capability to process particle rates up to 10^6 s^{-1} with high efficiency. Moreover ToF measurements should be feasible with resolutions well below 1 ns (FWHM).

These requirements can be met more easily by using scintillating fiber arrays being read out with position-sensitive photomultipliers than by using e.g. multi-wire gas chambers. Scintillating fiber detectors have experienced a rapid development in the last few years and have been established especially as tracking detectors in high-energy physics [3,4]. They are easy to operate, highly reliable, relatively insensitive to radiation damage and are very variable in the geometry of the detector, without the need of much material surrounding the active area.

Large area (50×50 cm^2) scintillating fiber detectors for relativistic heavy ions have been developed at GSI for experiments with the SIS accelerator. It is easier to detect heavy ions than minimum ionizing particles as in high energy physics, because the energy loss in matter increases with the square of the nuclear charge Z. On the other hand, a large dynamic range of light production for fragments of different nuclear charges has to be covered.

2 Description of the detector

The active area of the detector consists of about 500 parallel scintillating fibers (BCF-12 material [5]), covering 50×50 cm^2 as shown in Fig. 1. The fibers have a square cross section of 1×1 mm^2. The scintillating core of each fiber is coated by material of lower refraction index ("optical cladding" [5]) in order to guide the light. Cross talk between neighbouring fibers is avoided by an additional white coating ("extra mural absorber" [5]). Due to these parts of non-scintillating material the geometrical efficiency for particles impinging perpendicular to the area of the detector is reduced and can be estimated to be slightly below 90%.

In order to identify the fiber which was hit, one end of each fiber was coupled to a position-sensitive photomultiplier (PSPM) using a specially designed mask. For trigger purposes and to achieve good timing information the other ends of the fibers were read out by a conventional photomultiplier.

The PSPM Hamamatsu R3941 [6] has a rectangular 64×58 mm^2 photocathode and 16 mesh-type dynodes. The anode consists of a rectangular grid of 18 wires in one direction (x) and 16 wires in the orthogonal direction (y) with a distance

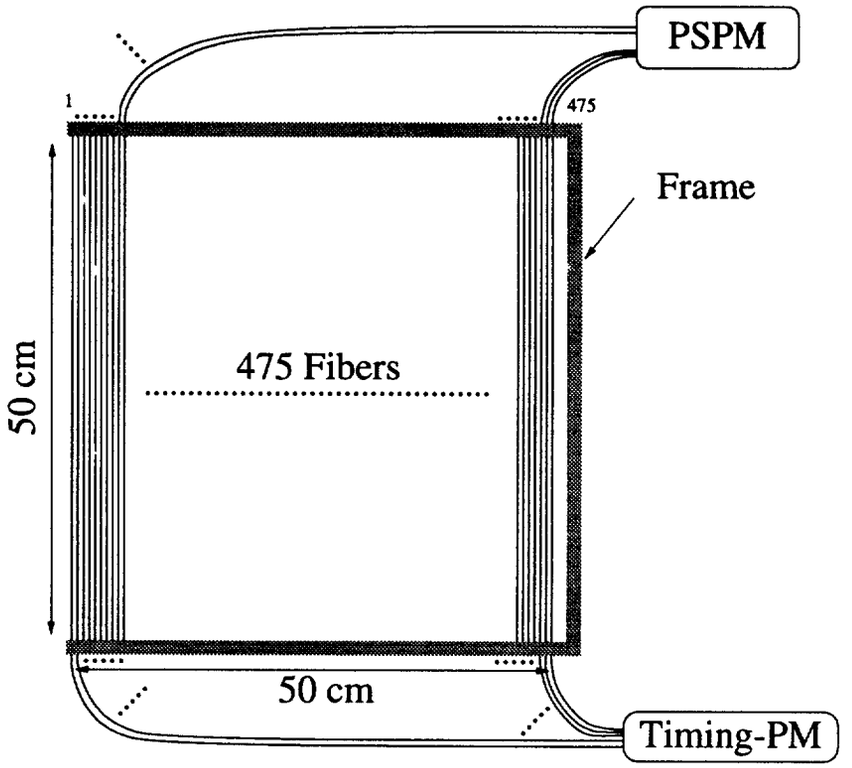

Fig. 1. Schematic view of the scintillating fiber detector. A total of 475 fibers are used, labelled from left to right as indicated. PSPM and timing-PM denote the photomultiplier used for the position and ToF measurements, respectively.

of approximately 3.7 mm between the anode wires. Due to this structure, the charge distribution on the anode grid is closely correlated with the position of the light spot on the photocathode. As will be shown below, a large number of fibers can be coupled to the photocathode and be identified this way. A PSPM with an anode grid is more suitable for such applications than an anode of pixel type (typically 16 to 256 pixels), because for the latter only one fiber can be read out per PSPM channel and the possible cross talk between neighbouring channels perturbs the reconstruction of the light incidence [7]. Moreover, for the pixel-type photomultiplier more electronic readout channels are needed. The pixel type PSPM, on the other hand, is suitable if the detector should recognize multihit events, while the present arrangement is restricted to applications where single hits are ensured.

In order to achieve a detector resolution corresponding to the width of the fibers, a safe identification of the hit scintillating fiber has to be achieved. For this purpose, the fibers were ordered in a matrix (see Fig. 2). As is indicated in the figure, some holes in the 25×20 mask used remain empty, because the number of fibers varies slightly from detector to detector. The distance from line to line and from column to column is 2.2 mm and 3.0 mm, respectively. The direction of placing the fibers in the matrix changes from line to line following a meander-like scheme. In order to obtain a safe identification, the

distance between lines of fibers on the PSPM was chosen wider than between columns, as a misinterpretation of fibers from different lines causes an error in position determination of the detector in the order of a few cm. Along a line, the distance may be shorter, depending on the number of fibers that are coupled to the PSPM, as a misinterpretation corresponds to a position error of only one fiber width (1 mm) on the detector.

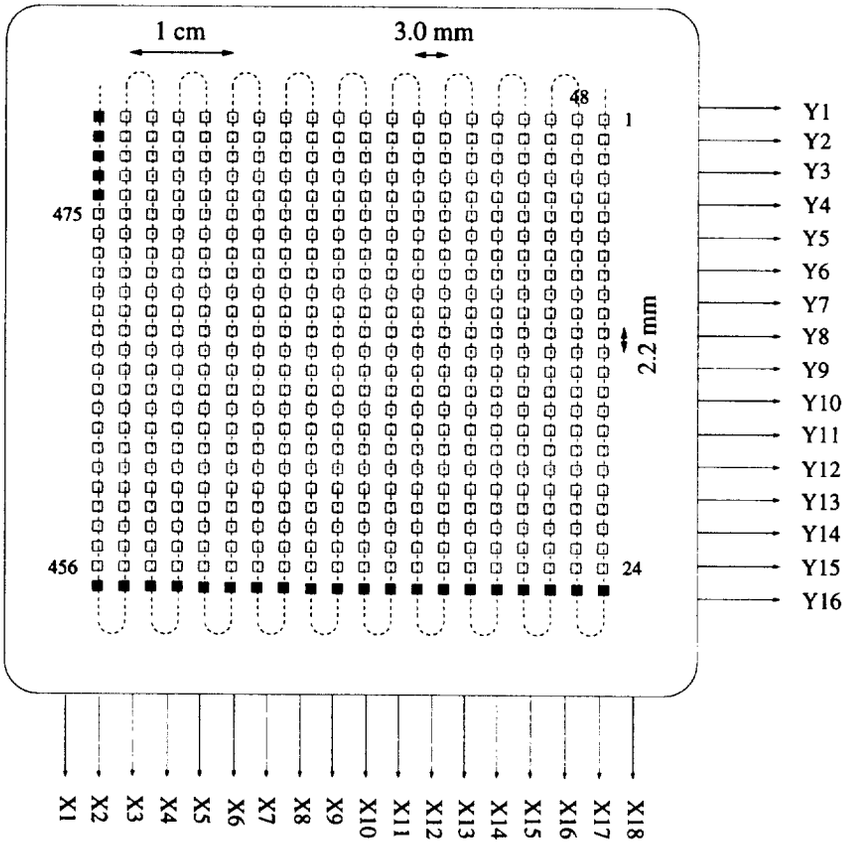

Fig. 2. Mask with 500 holes for fixing one end of the scintillating fibers to the position-sensitive photomultiplier (PSPM). Dark squares indicate unused holes, the meander-like ordering is indicated schematically by the dotted line (see text); numbers refer to the fiber labels as given in Fig. 1. The relative position of the anode wires of the PSPM are indicated as well.

3 Test measurements

In order to test the position resolution and linearity of the PSPM, its photocathode was systematically scanned with a light spot: the light of the scintillator was imitated using a nitrogen laser which emitted UV light (330 nm) in short pulses ($\sim$ 10 ns). The light was guided from the laser to the PSPM via a

glass fiber of diameter 0.2 mm and accurately positioned in x and y direction on the entrance window of the PSPM by means of a positioning device. The readout was done for every anode wire ("single-wire readout"), which allowed for a detailed look at charge distributions on the anode. The distributions exhibited a nearly gaussian shape, with a width of 3 to 4 wires (FWHM), slightly depending on the light intensity. The position of the light spot on the PSPM showed a good linear relation with the wire number for a large part of the photocathode (Fig. 3), where the measured position resolution reaches values down to 0.1 mm (FWHM), depending on the intensity of light.

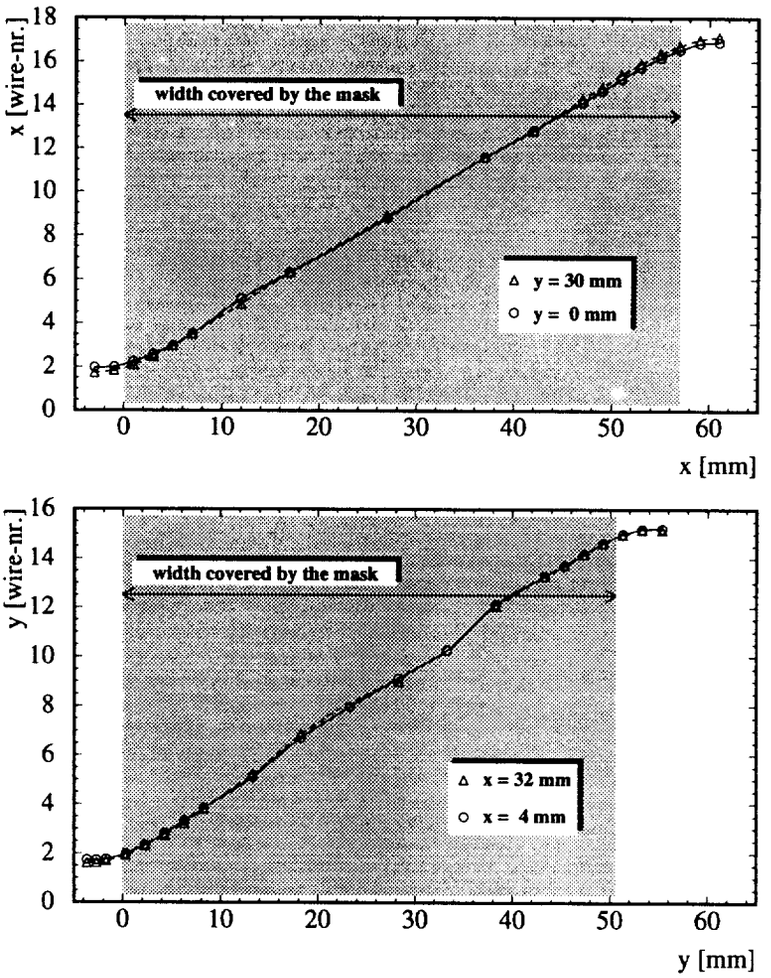

Fig. 3. Calibration curves for the readout of single anode wires: the centroid of the charge distribution is plotted versus the distance from the edge of the PSPM. The graphs show measurements parallel to the y-axis (upper diagram) and parallel to the x-axis (lower diagram) for a path through the middle (triangles), as well as along one edge (circles) of the PSPM. The errors are smaller than the symbols; the lines serve to guide the eye. The shaded regions indicate the width of the fiber mask in x and y direction. The offsets for the scales are chosen such that x=0 and y=0 correspond to the first row and first column of the mask, respectively.

A disadvantage of the single-wire readout is that it requires separate amplification and digitization of 34 signals per PSPM. In order to reduce the amount of data, two alternative methods can be applied: the anode wires (18 for x- and 16 for y-position) can be connected with chains of delay lines [3] or with chains of resistors [6], and only the signals of the ends of these chains (2×2 signals) have to be read out. The desired position information is then obtained by measuring the difference in time or difference in charge of the two signals per coordinate for the readout with delay chains or resistor chains, respectively.

For the PSPM R3941 used here, the width of the charge distribution was determined to be at least 3 wires in FWHM and about 8 wires in FWTM, corresponding to about 10 mm (FWHM) and about 30 mm (FWTM) on the photocathode, respectively. This is rather large, so that a position determination via delay line readout does not seem to be very promising. A rather narrow distribution of the order of 2 mm (FWHM) – as it was found in [3] and could be used to even disentangle double hits with a distance of $\gtrapprox$3 mm via delay-line readout – could not be observed.

In case of the readout via resistor chains, another disturbing effect was observed: anode wires being far away from the incidence of light show rather small signals, which are superimposed by induced positive signals. This happens mainly when the light is produced at an edge of the PSPM and it limits the position reconstruction via resistor-chain readout to the inner area of the PSPM, i.e. approximately 40×45 mm^2.

4 Experimental results

The scintillating fiber detector was operated with a variety of beams or fragments emerging from reactions from Hydrogen up to Uranium. The readout was done for every single anode wire after an amplification of the PSPM signals by a factor of 10 to 50. In order to determine the position of the ions passing through the detector, the location of the end of the scintillating fiber on the PSPM has to be determined from the charge distributions on the anode wires as mentioned above. If the centroid in x is plotted versus the centroid in y for each event, an image of the mask, through which the fibers are coupled to the PSPM, is produced. Fig. 4 shows examples for Xenon (700 A·MeV) and Lithium (457 A·MeV) beams. In order to identify the scintillating fiber, in the data analysis a grid is laid over this image and every point within one rectangle is assigned to a certain fiber. The mean positions of the peaks are hardly affected by the intensity of light detected, so that the calibration of the grid is rather stable. As long as the assignment is correct, the resolution of the detector is equal to the fiber width of 1 mm. The projections of one row and one column show an excellent separation of different fibers for the Xenon case.

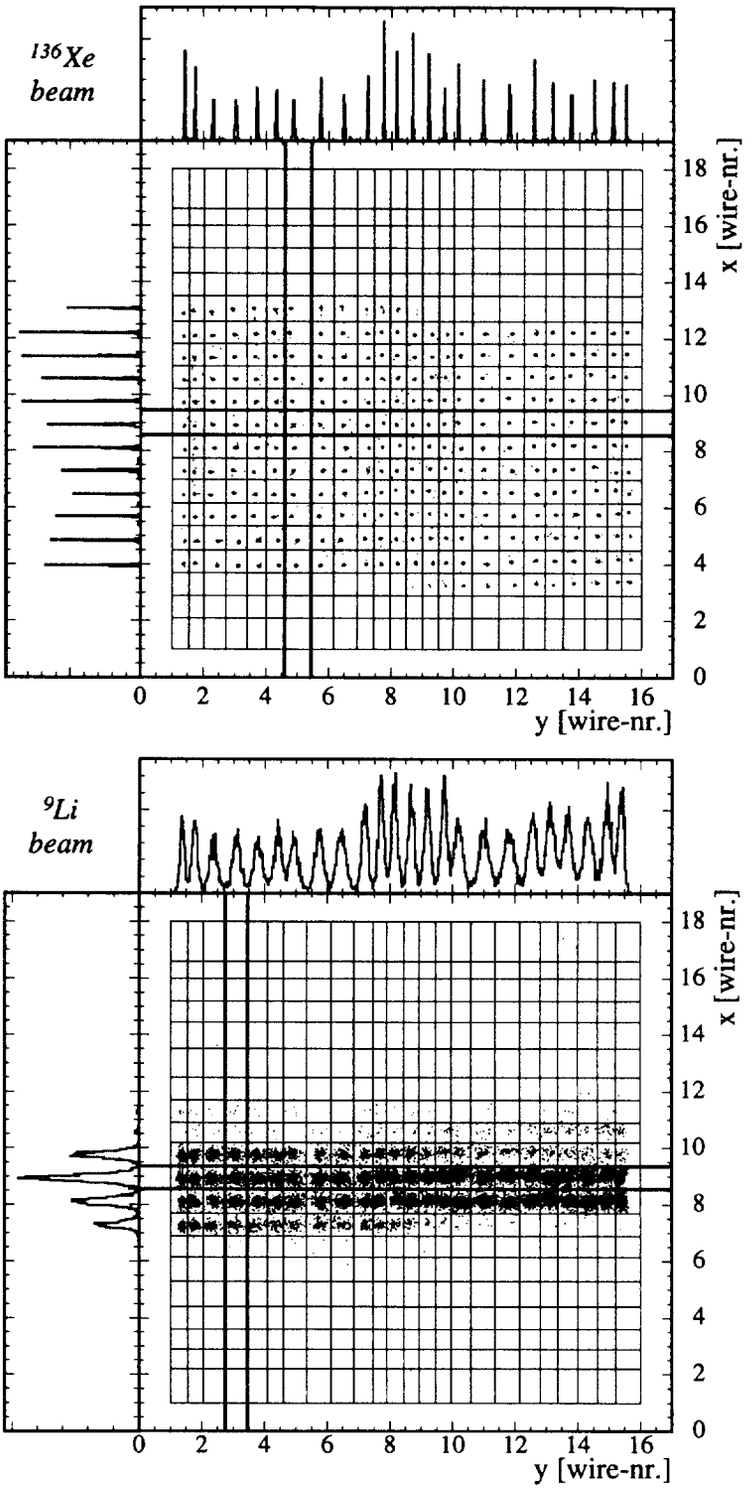

Fig. 4. Image of the fiber mask seen with a ^{136}Xe beam at 700 A·MeV (upper part) with a condition on a high sum energy deposited in the scintillator (see text) and of the fiber mask seen with a ^{9}Li beam at 457 A·MeV (lower part). Projections are shown on the upper and left side of each scatter plot for one row and one column, respectively, as indicated.

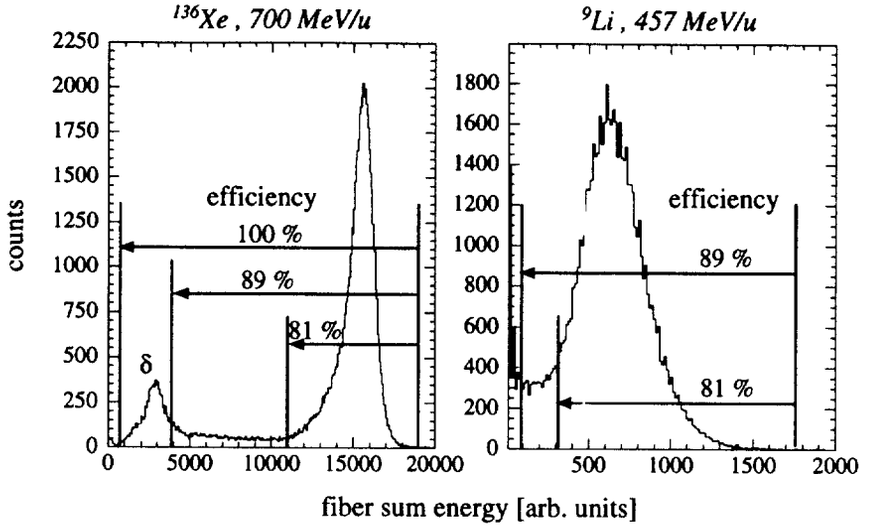

Fig. 5. Sum energy spectra for ^{136}Xe and ^{9}Li, corrected for the position dependence of the PSPM amplification. Detector efficiencies depending on the different thresholds in the sum energy are indicated. In the Xenon case, a peak appears at low energies, which is attributed to the energy loss of δ-electrons (see also text).

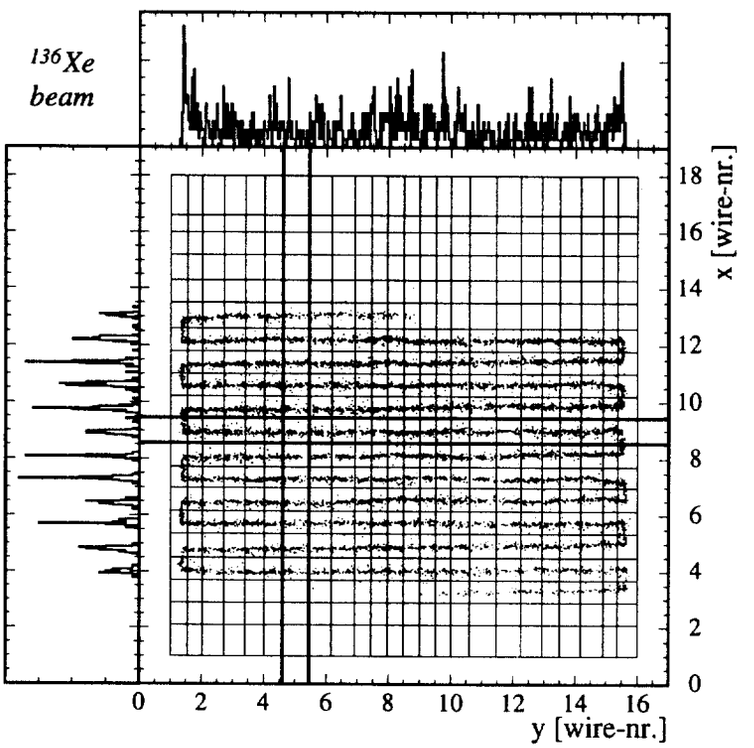

Fig. 6. Image of the fiber mask seen with a ^{136}Xe beam as in Fig. 4, but with a condition on the low-energy peak in the energy-sum spectrum attributed to δ-electrons, showing the meander-like ordering of the fibers in the mask.

For the Lithium case the resolution is just sufficient for a safe identification of the fiber row (3 mm distance between neighbouring rows), while within a row (2.2 mm distance), the peaks corresponding to the fibers are not completely separated, because of the smaller fiber distance in the mask.

In order to determine the efficiency of the detector it is convenient to evaluate the total energy deposited in the fibers, which was calculated by adding up the pulse heights of all 34 anode wires for each event. For one energy loss value (e.g. for Xenon ions of equal velocity) the PSPM amplification was found to vary about a factor of 3 depending on the position on the photocathode and, thus, depending on the fiber number. With such calibrations the energy sums could be corrected for position effects on the PSPM. The (corrected) sum-energy spectrum for Xenon ions (Fig. 5, left part) shows two broad peaks, one at high and one at low sum energies, while for projectiles with charge number $Z \lessapprox 10$, the low-energy peak is not separated from the noise, e.g. for Lithium ions (Fig. 5, right part). For the case of Xenon ions, the high sum-energy corresponds to the sharp peaks in the position determination (Fig. 4, upper part), while the low-energy peak corresponds to the positions in between (Fig. 6). The high-energy peak is attributed to the "normal" case where the ion traverses the scintillating core of one fiber. The valley between the two peaks is attributed to events where the ion traverses only part of the complete thickness of the scintillator. The low-energy peak is attributed to events where the heavy-ion projectile hits non-scintillating parts of the detector (cladding or absorber), but produces δ-electrons which hit the two neighbouring fibers simultaneously. For these events, the intensity of light produced in the fibers is much lower than in the case of one high-Z ion traversing one fiber. Consequently, the determination of the wire centroid leads to a value in between two fiber positions. The meander-like ordering of the fibers allows for a position reconstruction of such events even at the beginning or end of a row of fibers, as neighbouring fibers on the active area of the detector always have neighbouring positions on the PSPM (see Fig. 6 for illustration). Due to the effect of δ-electrons, it is possible to increase the detector efficiency, which is normally limited by the amount of active material seen by the ions, to nearly 100% for ions with $Z \gtrapprox 10$.

We find that the spatial resolution of the PSPM mainly depends on the amount of light produced in the fibers and only slightly on the position of the fiber on the photocathode. Typical resolutions for the inner part of the cathode are between 0.15 mm (FWHM) for Xenon and 0.9 mm for Lithium. Approaching the edges of the cathode, the resolution deteriorates to values between 0.21 mm (Xe) and 1.2 mm (Li) as shown in Fig. 7). In our setup, the lightest nuclei detectable (with position information) were Lithium ions at 457 A·MeV, depositing about 2.5 MeV energy in the scintillator, corresponding to $2 \cdot 10^4$ primary photons (8000 photons/MeV [5]). With a "trapping efficiency" to guide the light of 4%, an attenuation length of about 2 m, and a conversion

efficiency of the photocathode of about 20% the number of primary photoelectrons can be estimated to be of the order of 100 for the case of the Lithium beam. For Helium ions, the spatial resolution on the PSPM was found to be not sufficient for an unambiguous identification of the fibers, and for fast Hydrogen ions, being nearly minimum ionizing particles, the signals could not be isolated from the noise.

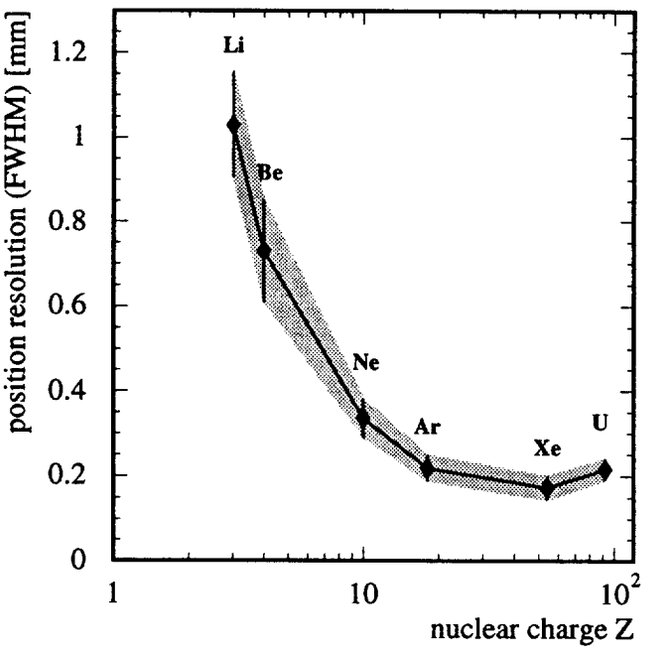

Fig. 7. Position resolution of the PSPM for projectiles of different charges corresponding to different amounts of light produced in the scintillating fibers. The bars indicate the variation of the resolution over the area of the photocathode.

The time resolution of the detector was measured versus other fast scintillation detectors in the path of the ions. The time signal was taken from a conventional 12-stage photomultiplier (Philips XP2262B) coupled to the end of the fibers opposite to the PSPM (see Fig. 1). The time resolution was found to improve from around 800 ps (FWHM) for Lithium ions to about 200 ps (FWHM) for Xenon ions. If good timing resolution is required and the particle distribution is extended in the direction parallel to the fibers, an additional position determination in this direction has to be performed by a supplementary detector in order to correct for the finite velocity of light expansion in the scintillator. This effect was corrected for in determining the above values for the time resolution.

5 Concluding remarks

For experiments with relativistic heavy-ion beams, a large area scintillating fiber detector has been developed. An array of approximately 500 fibers with 1×1 mm^2 square cross section was coupled to a position-sensitive photomultiplier (PSPM) via a mask. The fiber position on the PSPM was reconstructed by calculating the centroids of the charges collected from each wire of the anode grid. The accuracy achieved is sufficient for a safe identification of the fiber which was hit for projectiles with $Z \geq 3$, leading to a position resolution of the detector of 1 mm with the geometrical detector efficiency of 89%. The sensitivity could be increased down to Z=2 by coating the ends of the fibers opposite to the PSPM with a reflecting layer, thus increasing the available intensity of light nearly by a factor of 2, at the cost of abandoning the time measurement.

The detection of ions with $Z \gtrapprox 10$, on the one hand, allows to exploit the signals of their δ-electrons, thus increasing the detection efficiency to 100%, and on the other hand, would allow to read out even more fibers (up to 2000) with one single PSPM. This offers the possibility to implement much larger fiber arrays or to increase the position resolution of the detector by using thinner fibers.

Within the range of count rates used with the different beams no deterioration of the performance of the detector could be observed up to 10^5 particles per second. Higher count rates were not tested due to limitations of other detectors in the experiments, but, with the PSPM-signal lengths being about 10 ns and the total PSPM gain being relatively low ($\leq 10^6$) we expect that count rates up to 10^6 s^{-1} should be processed properly.

In conclusion, requirements for heavy-ion detection concerning spatial and time resolution, high detection efficiency and rate capability are met with such a detector. Moreover, it is easy to handle and stable in operation.

This work was supported by the German Ministry of Education and Research (BMBF) under Contracts 06 OF 474 and 06 MZ 465 and by GSI via Hochschulzusammenarbeitsvereinbarungen under Contracts OF ELK, MZ KRD, DA RIK and partly supported by the Polish Committee of Scientific Research under Contract PB2/P03B/113/02.

References

[1] K. Boretzky et al., Physics Letters B348 (1996) 30

[2] M. Zinser et al., Nucl. Phys. A619 (1997) 151

[3] V. Agoritsas et al., Nucl. Instr. and Meth. A357 (1995) 78

[4] V. Agoritsas et al., Nucl. Instr. and Meth. A372 (1996) 63

[5] Bicron Catalogue on Scintillating Optical Fibers

[6] Hamamatsu Technical Data Sheet on Position-Sensitive Photomultiplier Tubes with Crossed Wire Anodes (R3941 Series)

[7] J. Bähr et al., Nucl. Instr. and Meth. A348 (1994) 713